

# Calculation of muon transfer from muonic hydrogen to atomic oxygen

Arnaud Dupays, Bruno Lepetit, J. Alberto Beswick, Carlo Rizzo  
*Laboratoire Collisions, Agrégats, Réactivité, IRSAMC,  
 Université P. Sabatier, 31062 Toulouse, France*

Dimitar Bakalov  
*INRNE, Bulgarian Academy of Sciences, Sofia, Bulgaria  
 (Dated: January 16, 2022)*

The muon transfer probabilities between muonic hydrogen and an oxygen atom are calculated in a constrained geometry one dimensional model for collision energies between  $10^{-6}$  and  $10^3$  eV. For relative translational energies below  $10^{-1}$  eV, for which the de Broglie wavelength ( $> 1$  Å) is much larger than the characteristic distance of the potential interaction ( $\sim 0.1$  Å), the problem corresponds to an ultra-cold collision. The close-coupling time-independent quantum equations are written in terms of hyperspherical coordinates and a diabatic-by-sectors basis set. The muon transfer probabilities are qualitatively interpreted in terms of a model involving two Landau-Zener crossings together with the threshold energy dependence. Based on this analysis a simple procedure to estimate the energy dependence of the muon transfer rate in three dimensions, is proposed. These estimated rates are discussed in the light of previous model calculations and available experimental data for this process. It is concluded that the high transfer rates at epithermal energies inferred from experiments are unlikely to be correct.

## I. INTRODUCTION

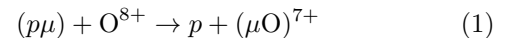
Negative muon transfer between exotic atoms (muonic hydrogen, for instance) and other atoms or molecules, has been extensively studied in the framework of muon catalysed nuclear fusion (see Ref. [1] and literature cited therein). Also, the structural and spectroscopic properties of these species is of interest for metrology as well as a test of quantum electrodynamic theories [2].

Very recently, a new method to measure the hyperfine structure ( $F = 0, 1$ ) of muonic hydrogen ( $p\mu$ ) based on the collisional energy dependence of muon transfer from the muonic hydrogen to an oxygen molecule, has been proposed [3]. When muonic hydrogen in the  $F = 0$  hyperfine ground state is laser excited to the  $F = 1$  level, collisions with  $H_2$  convert this excess energy into kinetic energy, giving an additional 0.12 eV translational energy to the muonic hydrogen. When the muon is transferred to an oxygen atom, it is captured in high ( $n = 5, 6$ ) states which promptly de-excite and emit X-rays. If the muon transfer rate to oxygen changes significantly from thermal (0.04 eV) to epithermal (0.16 eV) energies, the measurement of the X-ray emission intensity with and without laser excitation can be used for the determination of the hyperfine splitting in muonic hydrogen [2, 3]. This proposal was based on the work of Werthmüller *et al* [4] which indicates that muon transfer from hydrogen to oxygen increases by a factor of 3-4 going from thermal to epithermal collision energies.

While the experimental transfer rate at thermal energies have been borne out by the calculations of Sultanov and Adhikari [5], the rates at epithermal energies have never been confirmed theoretically. Even more, such an increase of the transfer rate with energy does not have a clear theoretical explanation. Werthmüller *et al* [4] suggest the existence of a resonance at low energies. It

is worth to stress that such an increase has not been observed in the case of muonic hydrogen colliding with sulfur [6] while for the case of  $CH_4$ , experimental data suggest that the transfer rate actually decreases going from thermal to epithermal energies [7]. In order to improve our understanding of this process and to assess the validity of the proposal of Ref. [3], it is important to perform model calculations to study in detail this reaction as a function of energy. It is the purpose of this paper to present such a study.

Since the muonic hydrogen has to approach one of the oxygen nuclei very close in order for the muon to transfer [8], the process can be described as



Although there have been several full three-dimensional calculations of muon transfer rates at low energies between muonic-hydrogen and low- $Z$  atoms (see literature cited in Ref. [9]), there is none when the transfer involves nuclei with  $Z > 3$ . There are several good reasons for that. As  $Z$  increases ( $Z = 8$  in our case) there is a larger initial-channel polarization and a stronger final-channels Coulomb interaction. In addition the number of open channels even at zero relative kinetic energy increases with  $Z$  making the full three-dimensional calculation very heavy. Thus up-to-now only approximate calculations have been performed for the muon transfer rate between muonic-hydrogen and oxygen [5, 8, 10]. Among them, the most recent and accurate is the one done by Sultanov and Adhikari [5], who used a two-channel approximation to the integro-differential Fadeev-Hahn formalism to calculate the muon transfer rates from muonic-hydrogen to the  $n = 5$  states of oxygen.

We have chosen to perform exact calculations but in a restricted configuration with the muon moving along

the line joining the proton to the oxygen atom. Indeed, for this system the colinear configuration is the most favorable for the transfer process. Furthermore, since the colinear configuration provides the minimum energy path for the reactance channel, even for an initial non colinear configuration there will be efficient orientational effects in particular for low translational energies.

Two model interaction potentials have been used in the calculations:

1. A pure coulombic potential with the bare oxygen nucleus  $O^{8+}$ .
2. A shorter range model potential with a distance dependent effective charge on the oxygen nucleus (calculated via a Thomas-Fermi electronic density model) to simulate the effect of the outer electrons.

The Hamiltonian was written in terms of hyperspherical coordinates. A piecewise diabatic basis set on the hyperspherical angle was used to expand the wave function. The basis functions have in turn been expanded in terms of first order Legendre functions to efficiently handle the two coulombic singularities at fixed hyperradii. The resulting close-coupling time-independent Schrödinger equations in the hyperradius were solved using a de Vogelaere algorithm and the partial and total muon transfer probabilities were determined by the standard S-matrix analysis at large distances. Since for energies below  $10^{-1}$  eV the muon transfer process studied here is equivalent to an ultra-cold collision (de Broglie wavelength ( $> 1$  Å) much larger than the characteristic distance ( $\sim 0.1$  Å) of the potential interaction), special care had to be taken to the asymptotic analysis in the reactant channel.

The paper is organized as follows. Section 2 introduces the model and the methodology used in the calculations. Section 3 presents the calculated muon transfer probabilities together with their interpretation in terms of simple Landau-Zener and threshold models. A procedure to estimate their energy behavior in the 3-dimensional case, is also presented. In section 4, the muon transfer rates are discussed in the light of previous model calculations and available experimental data for this process. Finally, section 5 is devoted to the conclusions.

## II. METHODOLOGY

The mass-scaled Jacobi coordinates adapted to the entrance channel of reaction (1) are :

$$R = \sqrt{\frac{m_{O,p\mu}}{m}} \left( x_O - \frac{m_\mu x_\mu + m_p x_p}{m_p + m_\mu} \right); \quad (2)$$

$$r = \sqrt{\frac{m_{p,\mu}}{m}} (x_\mu - x_p) \quad (3)$$

where

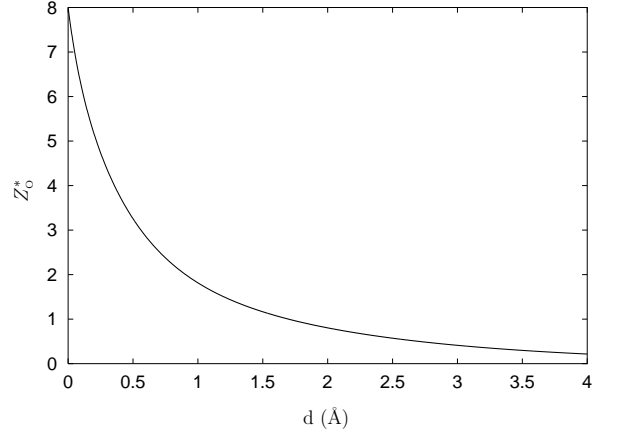


FIG. 1: Thomas-Fermi effective charge for the oxygen atom as a function of the distance to the  $O^{8+}$  nuclei.

$$m_{O,p\mu} = \frac{m_O (m_p + m_\mu)}{m_O + m_p + m_\mu}; \quad m_{p,\mu} = \frac{m_p m_\mu}{m_p + m_\mu}; \quad (4)$$

$$m = \left( \frac{m_O m_p m_\mu}{m_O + m_p + m_\mu} \right)^{1/2} \quad (5)$$

The hyperspherical coordinates are then defined by

$$\rho = \sqrt{R^2 + r^2}; \quad \tan \theta = r/R \quad (6)$$

where  $0 \leq \theta \leq \theta_\mu$ , with  $\theta_\mu = \arctan(m_\mu/m)$ . In terms of these coordinates and after regularisation of the wave function by the factor  $\sqrt{\rho}$  (the volume element is then given by  $d\rho d\theta$ ), the time-independent Schrödinger equation at total energy  $E$  is:

$$-\frac{\hbar^2}{2m} \left( \frac{\partial^2}{\partial \rho^2} + \frac{1}{\rho^2} \frac{\partial^2}{\partial \theta^2} \right) \psi(\rho, \theta) + \left( V(\rho, \theta) - \frac{\hbar^2}{8m\rho^2} - E \right) \psi(\rho, \theta) = 0 \quad (7)$$

where  $V(\rho, \theta)$  is the interaction potential given by

$$V = -\frac{e^2 Z_O^* (|x_\mu - x_O|)}{|x_\mu - x_O|} + \frac{e^2 Z_O^* (|x_p - x_O|)}{|x_p - x_O|} - \frac{e^2}{|x_p - x_\mu|} \quad (8)$$

Two sets of calculations have been performed. One with the bare oxygen nucleus, for which  $Z_O^* = 8$  in (8), and another with  $Z_O^*(d)$  being an effective charge given by the Thomas-Fermi model [11] and represented in Fig. 1.

The total wave function  $\psi(\rho, \theta)$  is expanded in terms of basis set wave functions depending on the hyperspherical angle  $\theta$ . We use a diabatic-by-sector representation. In

each sector  $\rho_n - \delta\rho_n \leq \rho < \rho_n + \delta\rho_n; n = 1, \dots, N_\rho$  we write:

$$\psi(\rho, \theta) = \sum_i F_i(\rho) \phi_i(\theta; \rho_n) \quad (9)$$

where  $\phi_i(\theta; \rho_n)$  are eigenstates of the Hamiltonian at fixed  $\rho_n$  distances. Their calculation requires the solution of a bound state problem for a potential showing Coulomb singularities at  $\theta = 0$  and  $\theta = \theta_\mu$ . Treatment of Coulomb singularities requires the use of specific methods such as increasing the density of grid points, or alternatively the oscillation frequency of the basis functions, near the singularities. Mapped Fourier [12, 13], Lagrange [14] or Schwartz [15, 16] interpolations are examples of such methods which have been used for cases with one singularity.

In our case we have two singularities to deal with at fixed hyperradius. Therefore we have used the auxilliary coordinate  $x = 2\theta/\theta_\mu - 1$ . This new variable is equivalent to one of the two hyperspherical elliptic angles [17], but constrained to be in the range  $[-1, 1]$  with the singularities being at the boundaries. If the  $\phi_i(\theta; \rho_n)$  functions are renormalized as:  $\phi_i(\theta; \rho) = (1 - x^2)^{\frac{1}{2}} \bar{\phi}_i(x; \rho)$ , both singularities of the potential are regularized. The  $\bar{\phi}_i(x; \rho)$  functions obey the differential equation:

$$\left( -\frac{2\hbar^2}{m\theta_\mu^2\rho^2} \hat{D} + (1 - x^2)(V - \frac{\hbar^2}{8m\rho^2}) \right) \bar{\phi}_i(x; \rho) = (1 - x^2)\epsilon_i(\rho)\bar{\phi}_i(x; \rho) \quad (10)$$

where

$$\hat{D} = (1 - x^2) \frac{\partial^2}{\partial x^2} - 2x \frac{\partial}{\partial x} - \frac{1}{1 - x^2} \quad (11)$$

Eq. 10 is solved by expanding  $\bar{\phi}_i(x; \rho)$  functions on the basis set of the eigenvectors of  $\hat{D}$ , which are the associated Legendre functions  $P_n^1(x)$ . This yields the generalized eigenvalue problem :

$$\left( -\frac{2\hbar^2}{m\theta_\mu^2\rho^2} \mathbf{D} + \mathbf{W} \right) \bar{\phi}_i(\rho) = \epsilon_i(\rho) \mathbf{O} \bar{\phi}_i(\rho) \quad (12)$$

where  $\bar{\phi}_i(\rho)$  is the vector of the unknown coefficients of the function  $\bar{\phi}_i(x; \rho)$  in the Legendre basis set. The matrix representation of the differential operator  $\mathbf{D}$  is diagonal, with diagonal elements  $-n(n+1)$ .  $\mathbf{W}$  is the potential coupling matrix and  $\mathbf{O}$  is the representation of  $(1 - x^2)$  in the Legendre basis. These matrices are calculated from a transformation of their diagonal representation in a grid of Gauss-Legendre quadrature points [18]. The system (12) is transformed to a standard eigenvalue problem after left multiplication by  $\mathbf{O}^{-\frac{1}{2}}$ . The method is expected to converge fast with the size of the basis set

(or equivalently with the number of grid points) since the use of a Gauss-Legendre scheme provides an adequately high density of points near  $x = \pm 1$ . Since the wavefunctions concentrate in the vicinity of  $x = \pm 1$  as energy decreases or as  $\rho$  increases, we expect convergence to be most difficult for lower levels and large  $\rho$ . At large  $\rho$ , we also expect convergence to be more difficult to achieve for  $O\mu$  states which are more compact than  $p\mu$  states. We have computed the relative error for a given number  $n_L$  of Legendre basis functions, using  $n_L = 450$  as a reference. For  $n_L = 150$ , we obtained 86 states converged better than  $10^{-8}$  of relative error up to  $\rho \sim a_0$ . For larger  $\rho$  values, the convergence starts to deteriorate, first for the ground state  $O\mu(n = 1)$ , then for the first excited state  $n = 2$  near  $\rho = 2a_0$ ... Using larger values of  $n_L$  delays the limit of convergence deterioration. For instance, with  $n_L = 250$ , the ground state is converged with  $10^{-8}$  relative precision up to  $\rho \sim 5a_0$ , up to  $\rho \sim 10a_0$  with  $n_L = 350$ . This latter value of  $n_L$  was used to generate the results shown below, and provided a basis converged better than  $10^{-4}$  up to  $\rho \sim 40a_0$  for all states except the first four ones which do not play any significant role in the charge transfer process considered here. As expected, among all these states, the ones corresponding to bound states of  $p\mu$  are the easiest to converge : the relative error at  $\rho = 40a_0$  for  $p\mu(n=1)$  is  $10^{-10}$  with  $n_L = 250$  and  $10^{-12}$  with  $n_L = 350$ . High accuracy on the  $p\mu(n = 1)$  channel is especially important for our present study since we consider initial relative kinetic energies as low as  $10^{-6}$  eV.

The close-coupling equations are integrated along the hyperradius  $\rho$  using the de Vogelaere algorithm [19]. In order to have convergence of the transfer probabilities to better than 1 % in the energy range considered here, we included 29 channels:  $((p\mu)_{n=1-4} + O \text{ and } p + (\mu O)_{n=1-25})$ . The integration of the coupled equations was performed from the origin to  $\rho_{\text{end}} \sim 30a_0$ .

The asymptotic analysis has been performed using the appropriate Jacobi coordinates for the entrance and for the product channels. The asymptotic states were expressed as products of Coulombic bound states and translational functions. For the product channels, the translational functions were approximated by simple plane waves. However, since the initial relative translational energy can be very small, the entrance channel has to be described with care to account for residual long range interactions. For the pure coulombic potential, this residual interaction has a  $1/R^2$  dependence (charge-dipole interaction). In this case, Bessel functions of imaginary order have been used as a basis set in  $R$ . For the screened Thomas-Fermi potential, wave functions depending on  $R$  have been numerically computed by inward integration from very large distances. These asymptotic wave functions and their derivatives are projected onto the hyperspherical basis functions  $\phi_i(x; \rho_{\text{end}})$  [19]. Transfer probabilities are then obtained by a standard S-matrix analysis.

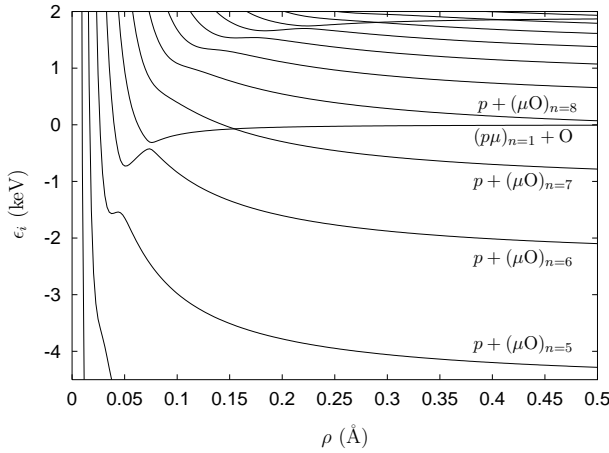


FIG. 2: Adiabatic energies as a function of the hyperradius.

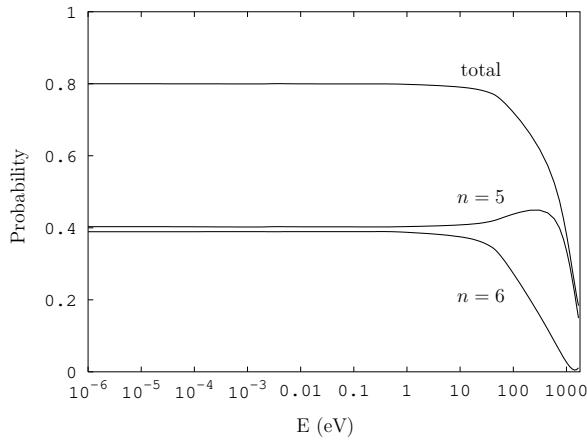


FIG. 3: Partial transfer probabilities calculated with the pure coulombic potential (bare oxygen nucleus).

### III. RESULTS OF THE CALCULATIONS

We have performed calculations for collision energies in the range  $10^{-6}$ – $10^3$  eV. In Fig. 2 we present the adiabatic energies  $\epsilon_i$  (see Eq. 10) as a function of the hyperradius  $\rho$ . The origin of energies has been chosen to coincide with the asymptotic limit of the entrance channel  $(p\mu)_{n=1} + O$ . Thus the calculations cover the energy range between this limit and the  $p + (\mu O)_{n=10}$  threshold.

The dynamics of muon transfer can be qualitatively understood by inspection of this figure. Starting in channel  $(p\mu)_{n=1} + O$ , the system crosses diabatically the channel  $p + (\mu O)_{n=7}$ . Muon transfer is completely negligible as the coupling is very small compared with the collision energy. The couplings to channels  $p + (\mu O)_{n=6}$  and  $p + (\mu O)_{n=5}$  are larger as evidenced by avoided crossings. The other channels  $p + (\mu O)_{n < 5}$  are weakly coupled to the initial one and they are not expected to be populated significantly.

In Figs. 3 and 4 we present the muon transfer proba-

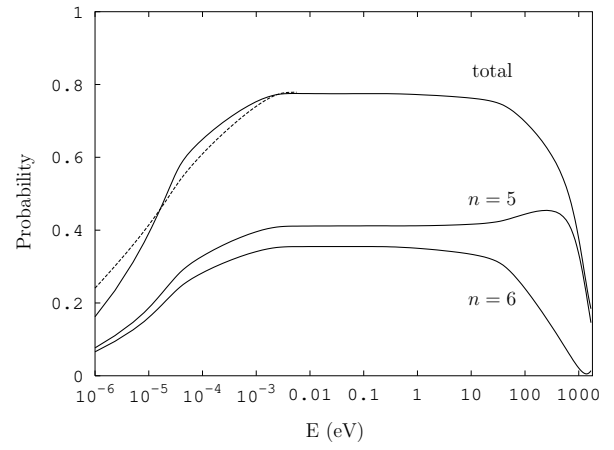


FIG. 4: Multichannel calculated partial and total transfer probabilities for the Thomas-Fermi potential. The dashed curve is the result of the Eq. (13)

bilities into the different product channels  $p + (\mu O)_{n=5,6}$  together with the total transfer probability, for the pure coulombic (C) and the Thomas-Fermi (TF) potentials, respectively. The two channels are about equally populated in both cases and the total transfer probability is high (80 %) for energies in the intermediate range (between  $10^{-2}$  and  $10^2$  eV). This can be understood in terms of non-adiabatic transitions in a simple 3 channels model ( $(p\mu)_{n=1} + O$  and  $p + (\mu O)_{n=6,5}$ ). Using the Landau-Zener expressions for the two crossings, a total transfer probability of  $\sim 0.6$  between 0 and  $10^2$  eV and a slow decrease at higher energies is obtained. This is in qualitative agreement with the fully converged results.

The main difference between the results for the C and TF potentials is at low energies. Whereas for the C potential the probabilities are constant at low energies, for the TF potential there is a typical threshold behavior. This is what is expected for short range potentials [11]. Indeed, in the colinear configuration the C potential behaves asymptotically as  $1/R^2$  (charge-dipole interaction) while the TF potential goes to zero much faster. At low energies, the amplitude of the wave function for  $1/R^2$  potentials near the origin is constant, while for short range potentials it decreases as energy goes to zero [11]. Thus the low energy dependence of the transfer probabilities is entirely determined by the asymptotic behavior of the potentials. This suggests that the dynamics can be described by a two step mechanism: a transmission in the incident channel through the long range part of the potential, followed by non adiabatic transitions in the interaction region. The charge transfer probability for low energies will be then given by

$$P(E) = |T(E)|^2 P_{max} \quad (13)$$

where  $T(E)$  is the transmittance in the incoming channel and  $P_{max}$  the plateau transfer probability.

The transmittance  $T(E)$  can be estimated by a simple one channel calculation with an effective potential of the

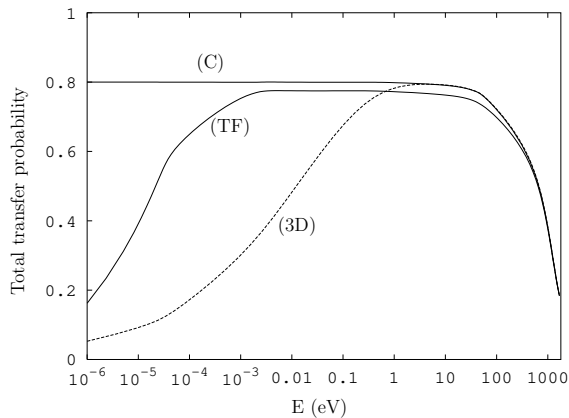


FIG. 5: Total transfer probabilities for the colinear model ((C): pure Coulombic potential, (TF): Thomas-Fermi model) and 3D estimate obtained from Eq. 13.

form

$$V_{\text{eff}}(R) = -\frac{\alpha Z_{\text{O}}^*(R)}{R^2}; \quad \alpha = \frac{3\hbar^2}{2m_{p,\mu}} \quad (14)$$

for  $R > R_0$  and  $V_{\text{eff}}(R) = V_{\text{eff}}(R_0)$  for  $R < R_0$ . The transfer radius has been taken at the avoided crossing with the  $p + (\mu\text{O})_{n=6}$  channel. For  $R < R_0$  the solution of this one-channel problem is given by

$$F(R) = T(E) \frac{\sin(KR)}{K^{1/2}} \quad (15)$$

with  $K = (2m_{\text{O},p\mu}(E - V_{\text{eff}}(R_0)))^{1/2}/\hbar$ , while for  $R \rightarrow \infty$  we have  $F(R) = \sin(kR + \delta)/k^{1/2}$  with  $k = (2m_{\text{O},p\mu}E)^{1/2}/\hbar$ . Numerical solution of the one channel problem thus provides directly  $T(E)$ . For the pure Coulombic potential ( $Z_{\text{O}}^* = 8$ ) we found  $T(E) = 1$ , consistent with the result of our multichannel calculations which gives a constant transfer probability at threshold (see Fig. 3). This unusual behavior is due to the particular  $1/R^2$  dependence of the effective potential [11]. The shorter range TF potential gives a more standard threshold behavior, with a transmittance going to 0 as energy decreases. This is apparent in Fig. 4 where the total transfer probabilities for the TF potential as a function of the energy are presented for both, the multichannel calculation and the simple estimation using Eq. (13). The two calculations agree within 10%.

This suggests a simple procedure for estimating the energy dependence in 3 dimensions (3D). In 3D, the ion-dipole interaction perturbs the  $p\mu_{n=1}$  initial state at second order through a  $-1/R^4$  term [8]. So even for the pure coulombic case there will be a threshold behavior at low energies. We have thus performed a one channel calculation of the transmittance  $T(E)$  with the 3D functional form of the potential. This  $T(E)$  was used in Eq. (13) together with  $P_{\text{max}}$  provided by the colinear Coulombic potential to yield an approximate 3-dimensional transfer

probability. Since the colinear configuration is the most favorable configuration, this procedure provides an upper limit of the total transfer probability. The results are presented in figure 5 together with those of the colinear calculations. Clearly, the threshold is displaced towards higher energies ( $10^{-1}$  eV). Thus we expect that for thermal energy collisions ( $4 \cdot 10^{-2}$  eV) the muon transfer probability will be of the order of 0.6 or less and will increase smoothly with energy in the range  $10^{-2} - 10^{-1}$  eV.

#### IV. DISCUSSION

In order to make contact with the experiments of Werthmüller *et al* [4], we have calculated the muon transfer rate according to:

$$\lambda(E) = N v \sigma(E) \quad (16)$$

with  $N$  being the number density of liquid hydrogen ( $4.25 \cdot 10^{22} \text{ cm}^{-3}$ ),  $v = \sqrt{2E/m_{\text{O},p\mu}}$  the relative velocity and

$$\sigma(E) = \frac{\pi}{k^2} P(E) \quad (17)$$

the muon transfer cross section with  $k = \sqrt{2m_{\text{O},p\mu}E}/\hbar$ . In writing Eq. (17), we have assumed only one partial wave with zero angular momentum. This is valid for collision energies up to 0.1–0.2 eV, corresponding to the height of the barrier in the entrance channel for the  $p$  partial wave.

In Fig. 6 we present our 3D estimates together with the results of the calculations of Sultanov and Adhikari [5] based on a two-states approximation of the Fadeev-Hahn equations. The agreement is good, our results being slightly higher than theirs. This was expected since our 3D estimation is based on the colinear calculations which provides an upper limit to the transfer probabilities. In addition, they have considered only the  $\text{O}\mu_{n=5}$  final channel. From Eqs. (16) and (17) it follows that for a constant transfer probability  $P(E) = 1$  the rate should decrease as  $1/\sqrt{E}$ . This is also plotted in Fig. 6. We note that our calculated rates decrease with energy slower than those for a constant transfer probability. The reason is that our calculated probabilities actually increase (although slower than  $1/\sqrt{E}$ ) in the energy range considered here as can be seen in Fig. 5.

In Fig. 6 we have also represented the rates of the two-component model used in Ref. [4] to fit the experimentally observed X-ray emission from excited muonic oxygen. While for thermal energies there is an order of magnitude agreement between our estimated values and the two-component model, there is a clear disagreement for epithermal energies. The two-component model predicts an increase of the rates going from thermal to epithermal energies in contradiction with our predictions and those of Sultanov and Adhikari [5]. Moreover, for energies

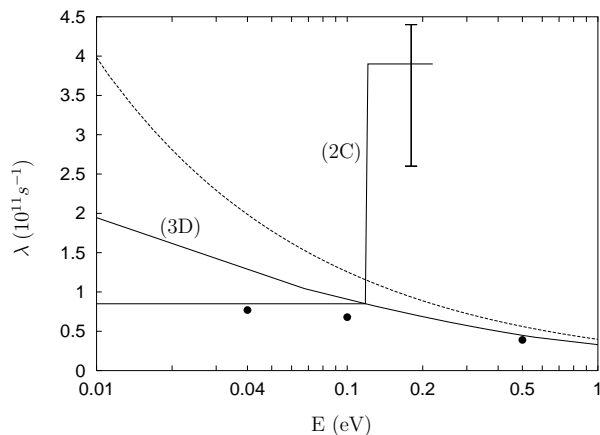


FIG. 6: Estimated transfer rates obtained in this work (3D). The dashed curve represents the rate corresponding to a maximum transfer probability  $P(E)$  of unity. The points are the calculated values of Sultanov and Adhikari [5] using the Fadeev formalism. The solid straight lines (2C) are the rates determined from fitting the experimental data of Ref. [4] with the two-component model.

above 0.1 eV the rate predicted by the two-component model is three times larger than the maximum values of the rate obtained by assuming a muon transfer probability per collision of unity (see Fig. 6).

## V. CONCLUSIONS

We have presented colinear calculations of muon transfer rates between muonic hydrogen and oxygen for relative translational energies between  $10^{-6}$  and  $10^3$  eV. For the lower energies (below  $10^{-1}$  eV) the de Broglie wavelength is much larger than the characteristic distance of the potential interaction and the problem corresponds to an ultra-cold collision. A simple procedure to estimate the energy dependence of the muon transfer rate in three dimensions was proposed.

Our results show that the muon transfer rate decrease going from thermal to epithermal energies, in agreement with previous theoretical calculations [5] but in contradiction with the assumptions of a two-component model used in Ref. [4] to interpret the experimental data on this system.

In the experiment the X-ray emission shows a bi-exponential behavior. In the two-component model of Werthmüller *et al* [4], it was assumed that the prompt emission is due to muon transfer from epithermal muonic hydrogen while the delayed emission, similar to what is observed when oxygen is replaced by other atoms, is associated to thermalized muonic hydrogen. Assuming that the relative amounts of epithermal and thermal species are equal, Werthmüller *et al* concluded that the rate of muon transfer from epithermal muonic hydrogen to oxygen should be larger than the one from thermalized ones

by a factor of almost 4. They suggest that a resonance could be responsible for this increase. We have shown that for s-waves it is not possible to obtain such an increase in the transfer rate, even if assuming a transfer probability per collision of one. Thus, if resonance effects exist they have to be due to the contribution of higher order partial waves. In an elastic cross section calculation, Kravtsov *et al* [20] have shown that for muonic hydrogen colliding with an oxygen nuclei, the contributions of  $p$  and  $d$  waves are small as compared to the  $s$  wave in the range 0–0.2 eV and that only at  $\sim 1.5$  eV there is narrow resonance involving the  $d$  wave. This will thus imply that the epithermal muonic hydrogen has much higher translational energy than what has been assumed in Ref. [4]. Anyway, this conclusion is based on a calculation of the elastic scattering. It could be of interest to check whether it is valid also for the muon transfer process as well.

In this work the calculations were performed in a restricted colinear configuration. This approximation is known to give poor quantitative results in many cases. However for the system considered here, the colinear configuration is the most favorable for the transfer process. Also, since the colinear configuration provides the minimum energy path for the reactance channel, even for an initial non colinear configuration there will be efficient orientational effects in particular for low translational energies. In addition we have introduced a correction to the low energy dependence of the rate in order to take into account the correct asymptotic behavior of the potential in 3-dimensions. Therefore, we believe that although quantitatively the results may change if a full 3-dimensional calculation is performed, the conclusions, in particular concerning the energy dependence of the muon transfer rates, will remain valid. A full 3-dimensional treatment is not impossible however, although quite computationally demanding. It will definitely be very important to further improve our detailed understanding of this reaction. It would also be most interesting to study the energy dependence of the muon-transfer rates for other elements, such as C or S, for which the rates seem to behave differently as a function of the energy. This work is in progress.

## VI. ACKNOWLEDGMENTS

We thank J.M. Launay for helpful discussions, the IDRIS for an allocation of CPU time on a NEC SX5 vector processor, and NATO for a collaborative linkage grant PST.CLG.978454 between Bulgaria and France.

- 
- [1] L. I. Ponomarev, *Hyp. Interact.* **138**, 15 (2001).
  - [2] D. Bakalov, E. Milotti, C. Rizzo, A. Vacchi, and E. Zavattini, *Phys. Lett. A* **172**, 277 (1993).
  - [3] A. Adamczak, D. Bakalov, K. Bakalova, E. Polacco, and C. Rizzo, *Hyp. Interact.* **136**, 1 (2001).
  - [4] A. Werthmüller, A. Adamczak, R. Jacot-Guillarmod, L. S. F. Mulhauser, L. Schellenger, H. Schneuwly, Y.-A. Thalmann, and S. Tresch, *Hyp. Interact.* **116**, 1 (1998).
  - [5] R. A. Sultanov and S. K. Adhikari, *Phys. Rev. A* **62**, 22509 (2000).
  - [6] F. Mulhauser and H. Schneuwly, *J. Phys. B: At. Mol. Opt. Phys.* **26**, 4307 (1993).
  - [7] K. Kirch, D. Abbott, B. Bach, P. Hauser, P. Indelicato, F. Kottmann, J. Missimer, P. Patte, R. T. Siegel, L. M. Simons, et al., *Phys. Rev. A* **59**, 3375 (1998).
  - [8] S. S. Gershtein, *Sov. Phys. JETP* **16**, 501 (1963), *zh. Eksp. Teor. Fiz.* **43**, 706 (1962).
  - [9] R. A. Sultanov and S. K. Adhikari, *J. Phys. B: At. Mol. Opt. Phys.* **35**, 935 (2002).
  - [10] P. K. Haff, E. Rodrigo, and T. A. Tombrello, *Ann. Phys.* **104**, 363 (1977).
  - [11] L. D. Landau and E. M. Lifshitz, *Quantum Mechanics* (Pergamon, Oxford, 1977).
  - [12] E. Fattal, R. Baer, and R. Kosloff, *Phys. Rev. E* **53**, 1217 (1996).
  - [13] D. Lemoine, *Chem. Phys. Lett.* **320**, 492 (2000).
  - [14] D. Baye and M. Vincke, *Phys. Rev. E* **59**, 7195 (1999).
  - [15] C. Schwartz, *J. Math. Phys.* **26**, 411 (1985).
  - [16] K. M. Dunseath, J. M. Launay, M. Terao-Dunseath, and L. Mouret, *J. Phys. B: At. Mol. Opt. Phys.* **35**, 3539 (2002).
  - [17] O. I. Tolstikhin, S. Watanabe, and M. Matsuzawa, *Phys. Rev. Lett.* **74**, 3573 (1995).
  - [18] G. C. Corey and D. Lemoine, *J. Chem. Phys.* **97**, 4115 (1992).
  - [19] B. Lepetit, J. M. Launay, and M. L. Dourneuf, *Chem. Phys.* **106**, 103 (1986).
  - [20] A. Kravtsov, A. Mikhailov, and N. Popov, *Phys. Lett. A* **223**, 129 (1996).